Flexible Transparent Conducting Hybrid Film Using a Surface-Embedded Copper Nanowire Network: A Highly Oxidation-Resistant Copper Nanowire Electrode for Flexible Optoelectronics

Hyeon-Gyun Im,[†,§] Soo-Ho Jung,[†,§,⊥] Jungho Jin,[†] Dasom Lee,[†] Jaemin Lee,[‡] Daewon Lee,[†] Jung-Yong Lee,[‡] Il-Doo Kim,[*,†] and Byeong-Soo Bae[*,†]

[†]Department of Materials Science and Engineering, Korea Advanced Institute of Science and Technology (KAIST), 291 Daehak-ro, Yuseong-gu, Daejeon 305-701, Republic of Korea and [‡]Graduate School of Energy, Environment, Water, and Sustainability (EEWS), Korea Advanced Institute of Science and Technology (KAIST), 291 Daehak-ro, Yuseong-gu, Daejeon 305-701, Republic of Korea. [§]H. G. Im and S. H. Jung contributed equally to this work. [⊥]Present address: (S.-H.J.): Korea Institute of Materials Science (KIMS), 797 Changwondaero, Seongsangu, Changwon, Gyeongnam 642-381, Republic of Korea.

ABSTRACT We report a flexible high-performance conducting film using an embedded copper nanowire transparent conducting electrode; this material can be used as a transparent electrode platform for typical flexible optoelectronic devices. The monolithic composite structure of our transparent conducting film enables simultaneously an outstanding oxidation stability of the copper nanowire network (14 d at 80 °C), an exceptionally smooth surface topography (R_{rms} < 2 nm), and an excellent opto-electrical performances (R_{sh} = 25 Ω sq^{-1} and T = 82%). A flexible organic light emitting diode device is fabricated on the transparent conducting film to demonstrate its potential as a flexible copper nanowire electrode platform.

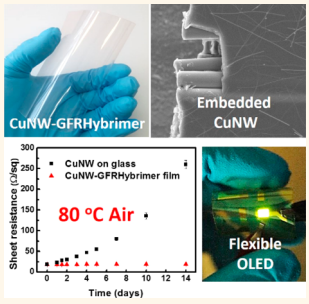

KEYWORDS: transparent conducting electrode · copper nanowire · flexible substrate · OLED

Metal nanowire (NW) is the most promising nanostructured transparent conducting electrode (TCE) material for the viable replacement of tin-doped indium oxide (ITO).[1−4] The key merits of metal NW as a TCE include its excellent opto-electrical property, large-scale fabrication based on solution process, and mechanical flexibility.[5,6] In particular, the outstanding flexibility is an important attribute of metal NW TCEs, making them well suited for use in flexible device applications. Typical flexible optoelectronic devices are fabricated using a plastic film—for example, PET—onto which a metal NW TCE is coated (hereafter, metal NW TCE/film platform).[7−14] Despite the large number of elaborations, however, it is not a simple task to prepare an optimized metal NW TCE/film platform that enables reproducible device fabrication and reliable performance. From a technical point of view, other than a mean opto-electrical property, a metal NW TCE/film platform should satisfy concurrently at least three key requirements: (1) a smooth surface topography, (2) strong adhesion between metal NW and substrate, and (3) overall high thermal/dimensional stability of the TCE/film platform. The intrinsic surface roughness that stems from the stacking or percolation of metal NW is one of the most critical sources of device failures such as short circuits and thus should be minimized (in general, roughness of a few nanometers is preferred).[8,10,11,15,16] Also, the metal NW TCE should remain tightly anchored on the film surface to avoid delamination of the NW from the underlying substrate.[17,18] Finally, the metal NW TCE/film platform should be robust enough in terms of

* Address correspondence to idkim@kaist.ac.kr, bsbae@kaist.ac.kr.

Received for review August 30, 2014 and accepted September 11, 2014.

Published online September 11, 2014
10.1021/nn504883m

thermal and dimensional stability because fabrication processes for typical optoelectronic devices generally involve high-temperature annealing steps.[11,19,20]

The two most intensively studied metal NW TCEs are the AgNW and the CuNW. To date, studies of the AgNW TCE have been numerous due to its excellent characteristics such as high electrical conductivity, commercial availability, and relatively higher oxidation resistance compared to the CuNW TCE.[15,17,21−23] Recently, however, CuNW TCEs have emerged as a potential contender for the replacement of both ITO and AgNW, which is mainly attributed to the CuNW's cost-effectiveness for performance: copper (ρ = 1.59 nΩ-m) has electrical conductivity comparable to that of silver (ρ = 1.67 nΩ-m), and yet it is 1000 times more abundant and 100 times less expensive than silver or indium.[24−27] CuNW TCEs have been fabricated with the aid of various fabrication techniques such as vacuum filtration,[28−30] spin coating,[31] spray deposition,[32] Meyer rod coating,[26] electro-spinning,[27] and electro-less deposition.[33] Although a number of state-of-the-art CuNW TCEs exhibiting opto-electrical performances comparable to those of ITO and AgNW TCE have been demonstrated, the intrinsically poor oxidation stability of the CuNW has been posed as the most critical drawback for its viable use.[34] Several proof-of-concept strategies have been suggested to address this issue. These include introducing inorganic encapsulation layers, for example, Ni or Ag, on the surface of individual CuNWs,[35−38] and additional overcoating layers, for example, graphene oxide, on an as-deposited CuNW network.[39,40] In one other approach, for example, Gao *et al*. recently reported that embedding a CuNW network on the surface of a polyacrylate can effectively improve the oxidation stability;[41] similar attempts have been made with AgNW and polymeric matrices such as poly(vinyl alcohol) and acrylate blends.[7,8,15,19]

Herein, we report a highly oxidation-resistant, high-performance CuNW TCE/film platform (CuNW−GFRHybrimer film). The CuNW−GFRHybrimer film features a CuNW TCE that is monolithically embedded on the surface of a transparent glass-fabric reinforced plastic (GFRHybrimer) film.[42] The resulting composite structure allows simultaneously an exceptional oxidation stability (14 d at 80 °C), a smooth surface topography (R_{rms} <2 nm), and tight anchoring of the CuNW TCE on the surface of the base film. In addition, the use of high-performance reinforced plastic film (the base GFRHybrimer film) can offer overall structural integrity allowing excellent thermal/dimensional stability and flexibility of the final CuNW−GFRHybrimer film. For the first time, we demonstrate the fabrication of a flexible organic light emitting diode (OLED) device using high-performance CuNW−GFHybrimer film as a TCE/film platform.

RESULTS AND DISCUSSION

As illustrated in Figure 1, a CuNW−GFRHybrimer film is produced by transferring a CuNW network, which is preformed on a donor glass, onto the surface of a base GFRHybrimer film *via* a vacuum-bag molding process, a typical fabrication setup for producing fiber-composite sheets. The CuNW used in this study is synthesized using a hydrazine-free method (Method section). Transmission electron microscopy (TEM) and X-ray diffraction (XRD) analyses of the CuNW confirm successful synthesis of the crystalline CuNW, showing characteristic diffraction patterns assigned to (111), (200), and (220) planes of the crystalline CuNW (Supporting Information, Figure S1). The average length and diameter of the CuNW are determined using multiple scanning electron microscopy (SEM) images (Supporting Information, Figure S2); average length and diameter values are found to be 35 μm and 50 nm, respectively.

The preformed CuNW network is coated on a donor glass substrate by both spray-deposition and vacuum filtration (Figure 1a). The spray deposition method is used for OLED fabrication because this process allows the formation of electrode patterns with the aid of a shadow mask. Otherwise, the vacuum filtration method is employed because it renders a CuNW network of higher purity. Prior to the CuNW deposition, the donor glass is surface-treated with octadecyltrichlorosilane to facilitate the release of the CuNW network in the subsequent transfer process. The preformed CuNW network is then annealed at 200 °C for 1 h under H_2 atmosphere (20% of H_2 and 80% of N_2). This annealing process allows effective reduction of the initial high junction resistance of the CuNW network, which is possibly caused by organic residues and/or a thin oxide layer (Supporting Information, Table S1).[32]

As schematically depicted in Figure 1c, the preformed CuNW network on the first donor glass (i) is brought into contact and compressed with the glass-fabric cloths impregnated with the matrix resin on the second donor glass (ii); this is followed by vacuum-bag molding and UV-curing (iii). During this process, the CuNW network is fully wetted and encased by the matrix resin, which allows the neat transfer of the CuNW network to the base film after UV-curing.[11] The matrix is a transparent resin blend consisting of cycloaliphatic epoxy oligosiloxanes (CAEO) and bis-[1-ethyl(3-oxetanyl)]methyl ether (DOX) as a functional cross-linker (Figure 1b). UV-curing of this CAEO/DOX blend renders a highly cross-linked hybrid thermoset that confers excellent thermal stability and oxidation resistance to the CuNW−GFRHybrimer film.[43] Finally, separation of the two donor glasses (iv) results in a transparent freestanding CuNW−GFRHybrimer film of which the thickness is ca. 60 μm (Figure 1d). The monolithic composite structure of the CuNW−GFRHybrimer film allows a tight encapsulation of the CuNW TCE with minimal out-of-plane exposure for electrical conduction, resulting in an exceptionally smooth surface topography (R_{rms} < 2 nm and

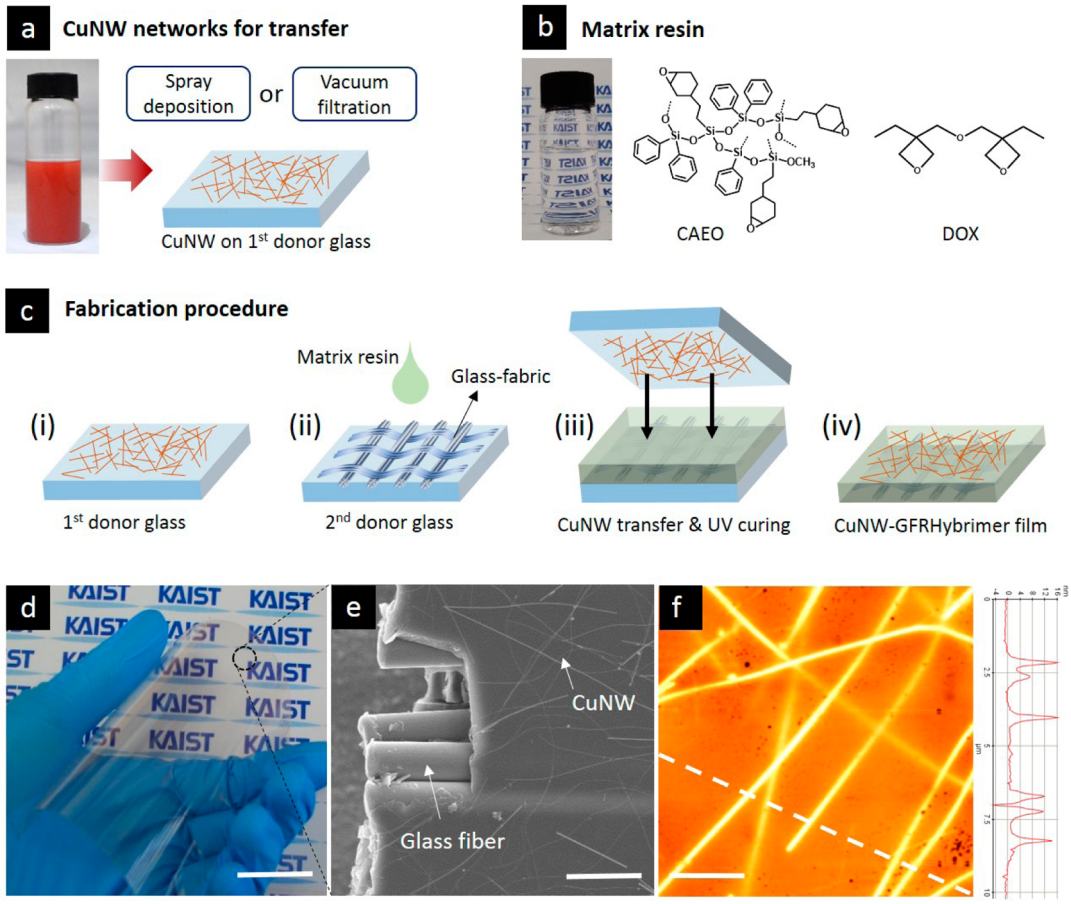

Figure 1. Fabrication of CuNW–GFRHybrimer film. (a) Preparation of a preformed CuNW network for transfer *via* spray-deposition or vacuum filtration. (b) A photograph of the matrix resin and chemical structures of the constituent CAEO (cycloaliphatic epoxy oligosiloxane) and DOX (bis[1-ethyl(3-oxetanyl)]methyl ether). (c) Fabrication procedure of CuNW–GFRHybrimer film. (d) A photograph of CuNW–GFRHybrimer film. The scale bar is 3 cm. (e) A surface SEM image of the CuNW–GFRHybrimer film, showing a monolithically embedded CuNW network on the base glass-fiber reinforced plastic film. The scale bar is 10 μm. (f) A topographic AFM image of CuNW–GFRHybrimer film. The right graph shows the contour profile of embedded CuNWs along the dashed line from the AFM image. The R_{rms} and peak-to-peak values are 2 and 16 nm, respectively (the scale bar is 2.5 μm).

maximum peak-to-peak value of ~16 nm) of the embedded CuNW TCE (Figure 1e, 1f and Supporting Information, Figure S3).

The mechanical durability of the TCE/film platform is of great importance in flexible optoelectronic devices. The bending test of the CuNW–GFRHybrimer film (R_{sh} = 35 Ω sq^{-1}) was evaluated using a lab-made bending test tool (Figure 2). The CuNW–GFRHybrimer film tolerates 10^4-times of bending cycles (bending radius of 5 mm) without any sign of mechanical failure while maintaining stability of electrical conduction, confirming the robust structural integrity of the CuNW–GFRHybrimer film. In contrast, the sheet resistance of the ITO deposited on the PEN (reference specimen, R_{sh} = 15 Ω sq^{-1}) sharply increased during the bending test.

The opto-electrical property of TCE is a pivotal figure of merit that determines the overall performance of a TCE. The total optical transmittance at 550 nm (T_{tot}) of CuNW–GFRHybrimer films with varying sheet resistance (R_{sh}) values are measured using a UV–vis spectrometer with ambient air baseline setting. This T_{tot} measurement with ambient air baseline setting gives the actual transmittance of a TCE/film platform and thus is of practical relevance. Figure 3 displays a plot of

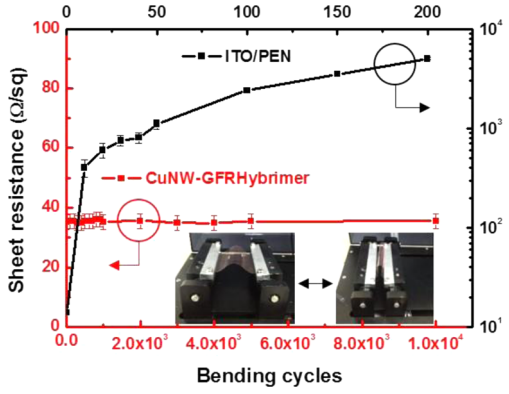

Figure 2. Bending test results of a CuNW–GFRHybrimer film (R_{sh} = 35 Ω sq^{-1}) and a reference ITO/PEN film (R_{sh} = 15 Ω sq^{-1}). Top and right axes are for the ITO/PEN (the inset represents the experimental setup for the bending test; bending radius is 5 mm).

T_{tot} *versus* R_{sh} for CuNW–GFRHybrimer films, where reference data sets from a number of recently reported CuNW TCEs are included for comparison (not all of the reference data sets are obtained with ambient air baseline setting, which may preclude explicit comparison).[26,28–30,32,41] Our CuNW–GFRHybrimer films show excellent opto-electrical performance, for example, R_{sh} = 25 Ω sq^{-1} and T_{tot} = 82% (Supporting Information, Table S2). It is worthwhile to note that the opto-electrical performances of the CuNW–GFRHybrimer films are comparable to or even, to some extent, superior to those of the current state-of-the-art CuNW TCEs of nonembedded type. The excellent opto-electrical performance of CuNW–GFRHybrimer film can be attributed to the improved contacts at the CuNW junctions, provided by the highly cross-linked rigid matrix.[11] For typical metal NW TCEs, the percolative figure of merit (Π) is often used to determine the opto-electrical performance; the Π value can be calculated using the following equation:[5,6]

$$T = \left[1+\frac{1}{\Pi}\left(\frac{Z_0}{R_{sh}}\right)^{1/(n+1)}\right]^{-2}$$

where T is the optical transmittance, Z_0 is the impedance of free space (377 Ω), and n is the percolation exponent. The higher Π and the smaller n are, the better the opto-electrical performance of a metal NW TCE will be. From Figure 3, the Π and the n values of the CuNW–GFRHybrimer film are 35 and 1, respectively.

Copper is prone to oxidation even at room temperature. The intrinsically poor oxidation resistance of CuNW has been regarded as the most critical drawback for this material's viable use as a flexible TCE. To highlight the superior thermal-oxidation stability of the CuNW–GFRHybrimer film, a series of thermal aging tests are performed (Figure 4). A CuNW–GFRHybrimer film (R_{sh} = 32 Ω sq^{-1}) is annealed on a hot-plate to 170 °C with a ramp rate of 5 °C min^{-1}; the R_{sh} of the film

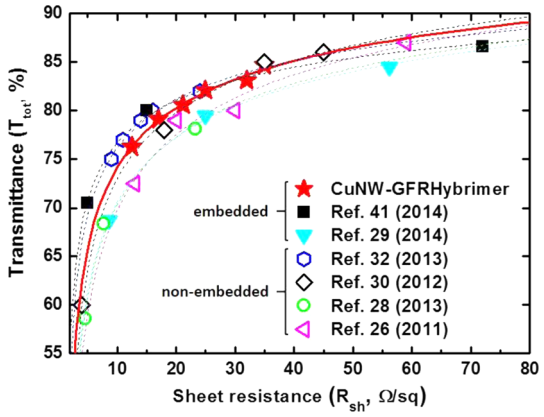

Figure 3. A plot of total optical transmittance at 550 nm (T_{tot}) as a function of sheet resistance (R_{sh}) for CuNW–GFRHybrimer films and several current state-of-art CuNW TCEs.

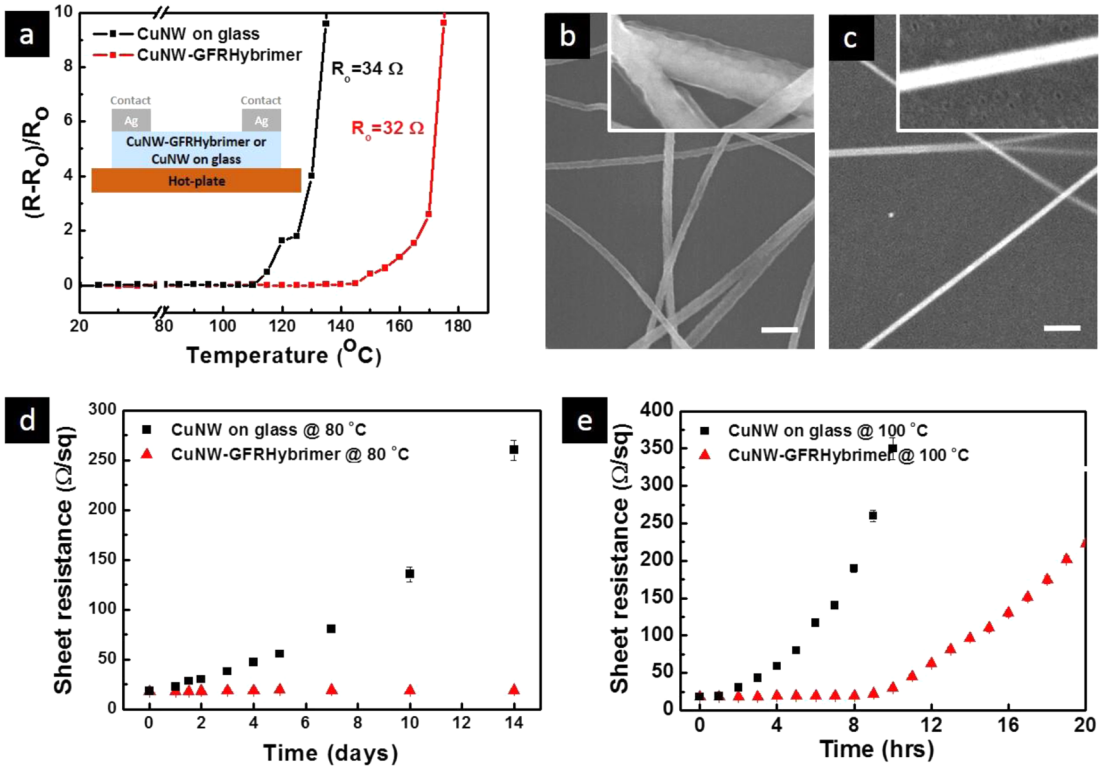

Figure 4. Thermal and oxidation stability of the CuNW–GFRHybrimer film. (a) A plot of normalized R_{sh} change ($R - R_o/R_o$) *vs* temperature (the inset scheme shows the experimental setup). Note that CuNW–GFRHybrimer film shows superior oxidation stability to the reference CuNW on glass. A surface SEM image, taken at 140 °C temperature point, of (b) the reference CuNW on glass showing oxidized CuNW and (c) the CuNW–GFRHybrimer film showing no signature of oxidation. The scale bars are 1 μm. (d, e) A plot of R_{sh} *vs* annealing period for the CuNW–GFRHybrimer film at 80 and 100 °C, respectively.

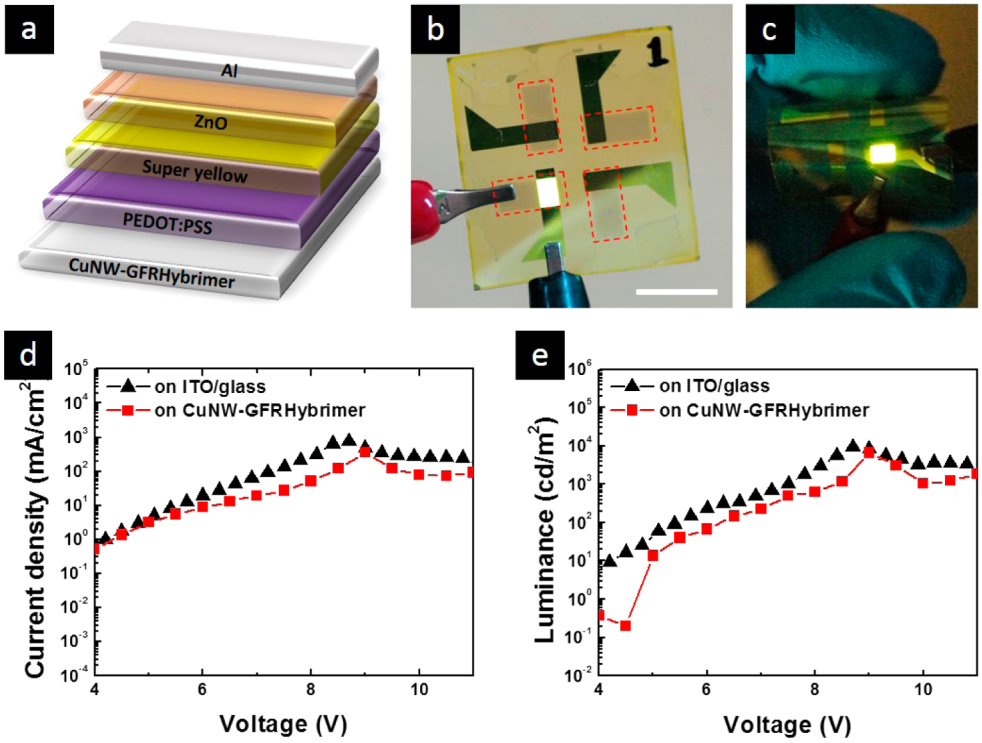

Figure 5. Demonstration of a flexible OLED on CuNW−GFRHybrimer film. (a) Device structure for the OLED. A photograph of the OLED device operating at (b) flat state (the dashed boxes show the patterned CuNW electrode directly produced by the transfer process) and (c) flexed state. The scale bar is 1 cm. (d) A plot of current density *vs* voltage (*J*−*V*). (e) A plot of luminance *vs* voltage (*L*−*V*). A reference OLED device on ITO/glass is tested for comparison.

is measured every minute (Figure 4a). For comparison, a reference sample of CuNW coated on a glass substrate (R_{sh} = 34 Ω sq^{-1}) is also tested. Two separate electrical outlets are formed on each sample with silver paste for the *in situ* R_{sh} measurement. It should be noted that R_{sh} of the reference CuNW on the glass substrate begins to increase catastrophically at 115 °C while the CuNW−GFRHybrimer film retains its initial R_{sh} even until 145 °C. Surface SEM analyses of the two samples taken at the 140 °C temperature point reveal a clear signature of thermal-oxidation for the CuNW on glass substrate and no distinct indication of thermal-oxidation for the CuNW−GFRHybrimer film (Figure 4 panels b and c, respectively). In the following experiment, the oxidation stability of the CuNW−GFRHybrimer film is further investigated. A CuNW−GFRHybrimer film (R_{sh} = 18 Ω sq^{-1}) and reference samples of CuNW on glass substrate (R_{sh} = 18 Ω sq^{-1}) are oven-annealed under ambient atmosphere at 80 and 100 °C (Figure 4 panels d and e, respectively). It should be noted that R_{sh} of the CuNW−GFRHybrimer film shows no significant change after a 14 d aging period at 80 °C. The electrical performance of CuNW−GFRHybrimer film is even stable until 8 h at 100 °C. In sharp contrast, the reference samples show immediate degradation of electrical performance at both 80 and 100 °C. The outstanding oxidation stability of the CuNW−GFRHybrimer film can be attributed to the structural morphology of the CuNW network. That is, monolithically embedded CuNW allows an optimal encapsulation of the CuNW network by the thermal-insulating matrix,[43] while providing minimal surface opening of CuNW for electrical conduction (Supporting Information, Figure S3).

The potential suitability of CuNW−GFRHybrimer film as a flexible TCE platform is demonstrated by fabricating an actual optoelectronic device (Figure 5). A solution-processed OLED with a typical bottom-emissive device structure is fabricated on a CuNW−GFRHybrimer film (R_{sh} = 21 Ω sq^{-1} and T_{tot} = 80%) (Figure 5a). Further details about the materials and fabrication procedures are described in the Method section. A windmill-shaped electrode pattern is produced on the CuNW−GFRHybrimer film by directly transferring a CuNW network identically predefined on a donor glass using a mask-assisted spray-deposition of CuNW solution (the dashed boxes shown in Figure 5b). This approach enables direct patterning of CuNW network into a desired geometry for the purpose of device interconnections.[44] The fabricated OLED device exhibits a stable operation even in a flexed state (Figure 5c). The characteristic current density−voltage (*J*−*V*) and luminance−voltage (*L*−*V*) curves of the OLED device and of a reference device fabricated on ITO/glass (sputtered ITO on glass substrate) (R_{sh} = 15 Ω sq^{-1} and T_{tot} = 85%) are shown in Figure 4 panels d and e, respectively. Although the OLED fabricated on the CuNW−GFRHybrimer film shows a small leakage current below 5 V in the *J*−*V* plot, both devices exhibit comparable performances.

This current leakage might possibly be due to interfacial defects at the CuNW/PEDOT:PSS interface which may have been created during the spin-coating of the hygroscopic PEDOT:PSS solution.[32] To the best of our knowledge, this is the first time that a flexible OLED device has been demonstrated using a CuNW TCE/film platform. On the basis of our results, we expect that CuNW−GFRHybrimer film can be a promising high-performance CuNW TCE/film platform for the fabrication of various flexible optoelectronics.

CONCLUSION

We have fabricated a flexible high-performance CuNW TCE/film platform (CuNW−GFRHybrimer film) that is suitable for flexible optoelectronic applications. The CuNW−GFRHybrimer film features a monolithically embedded CuNW TCE on a high-performance fiber-reinforced transparent plastic film. The CuNW−GFRHybrimer film exhibited excellent opto-electrical performance (R_{sh} = 25 Ω sq^{-1} and T = 82%) comparable to those of recent state-of-the-art CuNW TCEs, with superior mechanical flexibility. In particular, the monolithic hybrid structure enabled simultaneously an outstanding oxidation stability of the CuNW TCE and an exceptionally smooth surface topography. The potential suitability of CuNW−GFRHybrimer film as a TCE/film platform for flexible optoelectronics was here for the first time demonstrated in the fabrication of a typical OLED device. We believe that CuNW−GFRHybrimer film can be a promising candidate for the replacement of ITO and AgNW TCEs in optoelectronic applications.

METHODS

Synthesis of CuNW. Copper chloride (Sigma-Aldrich, 0.17 g) and glucose (Sigma-Aldrich, 0.1 g) were dissolved in 80 mL of distilled water. Hexadecylamine (Sigma-Aldrich, 1.44 g) was added to the solution slowly and mixed for 12 h with a magnetic stirrer. A light blue solution was then obtained, and the solution was placed in a Teflon-lined stainless steel autoclave. Without further stirring, the heating process was performed for 24 h at 120 °C. As a result, a reddish brown solution was obtained after the mixture was cooled to room temperature. The solution was then centrifuged (2000 rpm) for washing with distilled water, ethanol, and *n*-hexane, which was repeated for several times to remove the excess surfactant. The final product was then kept in *n*-hexane to avoid oxidation of the CuNW.

Deposition of CuNW on a Donor Glass and Postannealing Process. CuNW is deposited on a target substrate by two methods; vacuum filtration and spray deposition. For the vacuum filtration method, CuNWs dispersed in ethanol are filtered using a nylon membrane filter (0.2 μm pore, 47 mm-diameter). The filter was directly faced with a target substrate, and the CuNWs were transferred by using a compressor (only a few second of compressing is enough for the completion of transfer). For a large-scale deposition (10 × 10 cm^2) and electrode patterning, a CuNW solution (in ethanol) was sprayed using an automated spray-coater. The back pressure (N_2) was 0.1 MPa, and the flow rate of the CuNW solution was 3 mL min^{-1}. The nozzle-to-substrate distance was fixed to 13 cm, and the nozzle scan speed was 4000 in. min^{-1}. Temperature of the donor glass substrate was kept at 100 °C for an immediate solvent evaporation, and humidity in the spraying booth was maintained at 30%. Under the above specific conditions, for example, a CuNW network of 10 × 10 cm^2 in size and of 21 Ω sq^{-1} in sheet resistance could be prepared within a time frame of 1 min. (about five spraying cycles). Finally, the preformed CuNW on the donor glass was annealed using a tube furnace under H_2 atmosphere for 1 h at 200 °C.

Characterization. The sheet resistance (R_{sh}) was measured using a 4-point probe sheet resistance meter, and the measured R_{sh} values were also cross-checked using a multimeter. The SEM and TEM images were obtained using a scanning electron microscope (s4800, HITACHI) and a transmission electron microscope (Tecnai TF30 ST, FEI), respectively. XRD analysis was conducted using a multipurpose high power X-ray diffractometer (Rigaju, D/Max-2500). An atomic force microscopy (AFM) image was obtained using a scanning probe microscope (XE-100, Park systems).

OLED Fabrication. A 50 nm-thick PEDOT:PSS (Heraeus, PH-1000) was formed on the CuNW−GFRHybrimer by spin-coating and then preannealed at 120 °C on a hot-plate for 20 s. Subsequently, the film was postannealed at 120 °C inert atmosphere for 5 min to prevent oxidation of the CuNW TCE that may be caused by the acidic and hygroscopic PEDOT:PSS solution. A 60 nm-thick yellow light-emitting polymer (Merck, phenyl-substituted polyparaphenylenevinylene "Super Yellow," PDY-132) was spin-coated with spin-rate of 2500 rpm for 30 s. The ZnO nanoparticle layer (20 nm) was then spin-coated onto the emissive layer with a spin-rate of 3000 rpm for 30 s. The ZnO nanoparticle solution was synthesized by the method described by Beek *et al.*[45] Finally, Al electrodes (100 nm) were deposited using e-beam evaporation.

Conflict of Interest: The authors declare no competing financial interest.

Acknowledgment. This work was supported by the National Research Foundation of Korea (NRF) grant funded by the Korea government (MSIP) (CAFDC 5-3,NRF-2007-0056090 and Midcareer researcher program No. 2013R1A2A2A05005911). This work was also supported by the Center for Integrated Smart Sensors funded by the Ministry of Science, ICT & Future Planning as Global Frontier Project (CISS-2011-0031870)

Supporting Information Available: Detailed information on CuNW and CuNW−GFRHybrimer film. This material is available free of charge *via* the Internet at http://pubs.acs.org.

REFERENCES AND NOTES

1. Hu, L.; Wu, H.; Cui, Y. Metal Nanogrids, Nanowires, and Nanofibers for Transparent Electrodes. *MRS Bull.* **2011**, *36*, 760–765.
2. Hecht, D. S.; Hu, L.; Irvin, G. Emerging Transparent Electrodes Based on Thin Films of Carbon Nanotubes, Graphene, and Metallic Nanostructures. *Adv. Mater.* **2011**, *23*, 1482–1513.
3. Ellmer, K. Past Achievements and Future Challenges in the Development of Optically Transparent Electrodes. *Nat. Photonics* **2012**, *6*, 809–817.
4. Layani, M.; Kamyshny, A.; Magdassi, S. Transparent Conductors Composed of Nanomaterials. *Nanoscale* **2014**, *6*, 5581–5591.
5. De, S.; King, P. J.; Lyons, P. E.; Khan, U.; Coleman, J. N. Size Effects and the Problem with Percolation in Nanostructured Transparent Conductors. *ACS Nano* **2010**, *4*, 7064–7072.
6. De, S.; Coleman, J. N. The Effects of Percolation in Nanostructured Transparent Conductors. *MRS Bull.* **2011**, *36*, 774–781.
7. Gaynor, W.; Burkhard, G. F.; McGehee, M. D.; Peumans, P. Smooth Nanowire/Polymer Composite Transparent Electrodes. *Adv. Mater.* **2011**, *23*, 2905–2910.

8. Gaynor, W.; Hofmann, S.; Christoforo, M. G.; Sachse, C.; Mehra, S.; Salleo, A.; McGehee, M. D.; Gather, M. C.; Lussem, B.; Muller-Meskamp, L.; *et al*. Color in the Corners: ITO-Free White OLEDs with Angular Color Stability. *Adv. Mater.* **2013**, *25*, 4006–4013.
9. Lee, J.; Lee, P.; Lee, H. B.; Hong, S.; Lee, I.; Yeo, J.; Lee, S. S.; Kim, T. S.; Lee, D.; Ko, S. H. Room-Temperature Nanosoldering of a Very Long Metal Nanowire Network by Conducting-Polymer-Assisted Joining for a Flexible Touch-Panel Application. *Adv. Funct. Mater.* **2013**, *23*, 4171–4176.
10. Song, M.; You, D. S.; Lim, K.; Park, S.; Jung, S.; Kim, C. S.; Kim, D. H.; Kim, D. G.; Kim, J. K.; Park, J.; *et al*. Highly Efficient and Bendable Organic Solar Cells with Solution-Processed Silver Nanowire Electrodes. *Adv. Funct. Mater.* **2013**, *23*, 4177–4184.
11. Jin, J.; Lee, J.; Jeong, S.; Yang, S.; Ko, J.-H.; Im, H.-G.; Baek, S.-W.; Lee, J.-Y.; Bae, B.-S. High-Performance Hybrid Plastic Films: A Robust Electrode Platform for Thin-Film Optoelectronics. *Energy Environ. Sci.* **2013**, *6*, 1811–1817.
12. Choi, D. Y.; Kang, H. W.; Sung, H. J.; Kim, S. S. Annealing-Free, Flexible Silver Nanowire-Polymer Composite Electrodes *via* a Continuous Two-Step Spray-Coating Method. *Nanoscale* **2013**, *5*, 977–983.
13. Lee, M. S.; Lee, K.; Kim, S. Y.; Lee, H.; Park, J.; Choi, K. H.; Kim, H. K.; Kim, D. G.; Lee, D. Y.; Nam, S.; *et al*. High-Performance, Transparent, and Stretchable Electrodes Using Graphene-Metal Nanowire Hybrid Structures. *Nano Lett.* **2013**, *13*, 2814–2821.
14. Yang, L.; Zhang, T.; Zhou, H.; Price, S. C.; Wiley, B. J.; You, W. Solution-Processed Flexible Polymer Solar Cells with Silver Nanowire Electrodes. *ACS Appl. Mater. Interfaces* **2011**, *3*, 4075–4084.
15. Yun, S.; Niu, X.; Yu, Z.; Hu, W.; Brochu, P.; Pei, Q. Compliant Silver Nanowire-Polymer Composite Electrodes for Bistable Large Strain Actuation. *Adv. Mater.* **2012**, *24*, 1321–1327.
16. Müllen, K.; Scherf, U.: *Organic Light Emitting Devices: Synthesis, Properties and Applications*; Wiley-VCH Verlag: Weinheim, Germany, 2006.
17. Amjadi, M.; Pichitpajongkit, A.; Lee, S.; Ryu, S.; Park, I. Highly Stretchable and Sensitive Strain Sensor Based on Silver Nanowire-Elastomer Nanocomposite. *ACS Nano* **2014**, *8*, 5154–5163.
18. Lee, J.; Lee, I.; Kim, T. S.; Lee, J. Y. Efficient Welding of Silver Nanowire Networks without Post-Processing. *Small* **2013**, *9*, 2887–2894.
19. Zeng, X. Y.; Zhang, Q. K.; Yu, R. M.; Lu, C. Z. A New Transparent Conductor: Silver Nanowire Film Buried at the Surface of a Transparent Polymer. *Adv. Mater.* **2010**, *22*, 4484–4488.
20. Im, H.-G.; Jin, J.; Ko, J.-H.; Lee, J.; Lee, J.-Y.; Bae, B.-S. Flexible Transparent Conducting Composite Films Using a Monolithically Embedded AgNW Electrode with Robust Performance Stability. *Nanoscale* **2013**, *6*, 711–715.
21. Koga, H.; Nogi, M.; Komoda, N.; Nge, T. T.; Sugahara, T.; Suganuma, K. Uniformly Connected Conductive Networks on Cellulose Nanofiber Paper for Transparent Paper Electronics. *NPG Asia Mater.* **2014**, *6*, e93.
22. Lee, J. Y.; Connor, S. T.; Cui, Y.; Peumans, P. Solution-Processed Metal Nanowire Mesh Transparent Electrodes. *Nano Lett.* **2008**, *8*, 689–692.
23. Hu, L.; Kim, H. S.; Lee, J. Y.; Peumans, P.; Cui, Y. Scalable Coating and Properties of Transparent, Flexible, Silver Nanowire Electrodes. *ACS Nano* **2010**, *4*, 2955–2963.
24. *Mineral Commodity Summaries*; U.S. Geological Survey: Reston, VA, 2014.
25. Rathmell, A. R.; Bergin, S. M.; Hua, Y. L.; Li, Z. Y.; Wiley, B. J. The Growth Mechanism of Copper Nanowires and Their Properties in Flexible, Transparent Conducting Films. *Adv. Mater.* **2010**, *22*, 3558–3563.
26. Rathmell, A. R.; Wiley, B. J. The Synthesis and Coating of Long, Thin Copper Nanowires to Make Flexible, Transparent Conducting Films on Plastic Substrates. *Adv. Mater.* **2011**, *23*, 4798–4803.
27. Wu, H.; Hu, L.; Rowell, M. W.; Kong, D.; Cha, J. J.; McDonough, J. R.; Zhu, J.; Yang, Y.; McGehee, M. D.; Cui, Y. Electrospun Metal Nanofiber Webs as High-Performance Transparent Electrode. *Nano Lett.* **2010**, *10*, 4242–4248.
28. Guo, H.; Lin, N.; Chen, Y.; Wang, Z.; Xie, Q.; Zheng, T.; Gao, N.; Li, S.; Kang, J.; Cai, D.; et al. Copper Nanowires as Fully Transparent Conductive Electrodes. *Sci. Rep.* **2013**, *3*, 2323.
29. Hu, W.; Wang, R.; Lu, Y.; Pei, Q. An Elastomeric Transparent Composite Electrode Based on Copper Nanowires and Polyurethane. *J. Mater. Chem. C* **2014**, *2*, 1298–1305.
30. Zhang, D.; Wang, R.; Wen, M.; Weng, D.; Cui, X.; Sun, J.; Li, H.; Lu, Y. Synthesis of Ultralong Copper Nanowires for High-Performance Transparent Electrodes. *J. Am. Chem. Soc.* **2012**, *134*, 14283–14286.
31. Li, S.; Chen, Y.; Huang, L.; Pan, D. Large-Scale Synthesis of Well-Dispersed Copper Nanowires in an Electric Pressure Cooker and Their Application in Transparent and Conductive Networks. *Inorg. Chem.* **2014**, *53*, 4440–4444.
32. Sachse, C.; Weiß, N.; Gaponik, N.; Müller-Meskamp, L.; Eychmüller, A.; Leo, K. ITO-Free, Small-Molecule Organic Solar Cells on Spray-Coated Copper-Nanowire-Based Transparent Electrodes. *Adv. Energy Mater.* **2014**, *4*, 1300737.
33. Hsu, P. C.; Kong, D.; Wang, S.; Wang, H.; Welch, A. J.; Wu, H.; Cui, Y. Electrolessly Deposited Electrospun Metal Nanowire Transparent Electrodes. *J. Am. Chem. Soc.* **2014**, *136*, 10593–10596.
34. Han, S.; Hong, S.; Ham, J.; Yeo, J.; Lee, J.; Kang, B.; Lee, P.; Kwon, J.; Lee, S. S.; Yang, M. Y.; *et al*. Fast Plasmonic Laser Nanowelding for a Cu-Nanowire Percolation Network for Flexible Transparent Conductors and Stretchable Electronics. *Adv. Mater.* **2014**, 10.1002/adma.201400474.
35. Hsu, P. C.; Wu, H.; Carney, T. J.; McDowell, M. T.; Yang, Y.; Garnett, E. C.; Li, M.; Hu, L.; Cui, Y. Passivation Coating on Electrospun Copper Nanofibers for Stable Transparent Electrodes. *ACS Nano* **2012**, *6*, 5150–5156.
36. Rathmell, A. R.; Nguyen, M.; Chi, M.; Wiley, B. J. Synthesis of Oxidation-Resistant Cupronickel Nanowires for Transparent Conducting Nanowire Networks. *Nano Lett.* **2012**, *12*, 3193–3199.
37. Stewart, I. E.; Rathmell, A. R.; Yan, L.; Ye, S.; Flowers, P. F.; You, W.; Wiley, B. J. Solution-Processed Copper-Nickel Nanowire Anodes for Organic Solar Cells. *Nanoscale* **2014**, *6*, 5980–5988.
38. Luo, X.; Gelves, G. A.; Sundararaj, U.; Luo, J. L. Silver-Coated Copper Nanowires with Improved Anti-oxidation Property as Conductive Fillers in Low-Density Polyethylene. *Can. J. Chem. Eng.* **2013**, *91*, 630–637.
39. Won, Y.; Kim, A.; Lee, D.; Yang, W.; Woo, K.; Jeong, S.; Moon, J. Annealing-Free Fabrication of Highly Oxidation-Resistive Copper Nanowire Composite Conductors for Photovoltaics. *NPG Asia Mater.* **2014**, *6*, e105.
40. Kholmanov, I. N.; Domingues, S. H.; Chou, H.; Wang, X.; Tan, C.; Kim, J. Y.; Li, H.; Piner, R.; Zarbin, A. J. G.; Ruoff, R. S. Reduced Graphene Oxide/Copper Nanowire Hybrid Films as High-Performance Transparent Electrodes. *ACS Nano* **2013**, *7*, 1811–1816.
41. Sun, J.; Cheng, Y.; Wang, S.; Wang, R.; Gao, L. Copper Nanowire Based Transparent Conductive Films with High Stability and Superior Stretchability. *J. Mater. Chem. C* **2014**, *2*, 5309–5316.
42. Jin, J.; Ko, J. H.; Yang, S.; Bae, B. S. Rollable Transparent Glass-Fabric Reinforced Composite Substrate for Flexible Devices. *Adv. Mater.* **2010**, *22*, 4510–4515.
43. Yang, S. C.; Jin, J. H.; Kwak, S.-Y.; Bae, B.-S. Thermo-Mechanical/Thermal Properties of Photo-cationic Polymerized Cyclo-aliphatic Epoxy Hybrid Materials. *Macromol. Res.* **2011**, *19*, 1166–1171.
44. Hecht, D. S.; Thomas, D.; Hu, L.; Ladous, C.; Lam, T.; Park, Y.; Irvin, G.; Drzaic, P. Carbon-Nanotube Film on Plastic as Transparent Electrode for Resistive Touch Screens. *J. Soc. Info. Display* **2009**, *17*, 941.
45. Beek, W. J. E.; Wienk, M. M.; Kemerink, M.; Yang, X.; Janssen, R. A. J. Hybrid Zinc Oxide Conjugated Polymer Bulk Heterojunction Solar Cells. *J. Phys. Chem. B* **2005**, *109*, 9505–9516.